TURBOMACHINERY & PUMP SYMPOSIA | HOUSTON, TX
AUGUST 20-22, 2024
SHORT COURSES: AUGUST 19, 2024

THRUST BEARING FAILURE IN A LARGE LNG REFRIGERATION COMPRESSOR

Ed Wilcox
Senior Principal Machinery Engineer
Chevron Technology Center
Houston, TX, USA

Matthew Marchione
Chief Engineer Aftermarket
Kingsbury, Inc
Philadelphia, PA, USA

Bruce R. Fabijonas
Research & Development Manager
Kingsbury, Inc.
Philadelphia, PA, USA

Ed Wilcox is a Senior Principal Machinery Engineer with Chevron Technology Center(CTC). He has 34 years of machinery experience and is the Global Technical Authority for Rotating Equipment within Chevron. Likewise, he is currently the Chairman of the API SOME Steering Committee. Prior to his Chevron career, he worked for Conoco and Lyondell Chemical as a machinery engineer. He has a BSME degree from the University of Missouri-Rolla and an MSME degree from Oklahoma State University. He is a Vibration Institute Category IV Vibration Specialist and a registered Professional Engineer in the State of Oklahoma.

Matthew Marchione holds the position of Chief Engineer – Aftermarket at Kingsbury, Inc, where he has worked for 35 years. He is responsible for the design, analysis, distress evaluation and repair of fluid-film thrust and journal bearings. Prior to Kingsbury, he worked for Vibration Specialty Corporation and Mechanical Technology Inc., where he performed field service and analytical studies aimed at eliminating industrial machine vibration. He earned his BS from Villanova University (General Science, 1980).

Bruce Fabijonas is Manager of Research and Development at Kingsbury, Inc. He oversees Kingsbury's suite of test rigs and is responsible for Kingsbury's bearing analysis software. He earned his PhD from the University of Illinois Chicago (Applied Mathematics, 1997) and is a member of STLE.

ABSTRACT

A large LNG refrigeration compressor application recently experienced multiple thrust bearings failures on two identical machines. Analysis of the thrust load during normal operation showed that the thrust bearing was very lightly loaded, less than 20% of the bearing's design capacity. This was confirmed by low thrust position and thrust bearing temperatures. Several alternate theories were evaluated including inadequate lubrication and worn compressor labyrinths, but none proved to be correct. A thorough calculation of the thrust

loads by the compressor OEM and the operator, accounting for a variable pressure profile on both sides of the compressor impellers and worn division wall labyrinths also showed only acceptable amounts of thrust load. Analysis of the transient load during upset shutdown conditions by the operator revealed that the thrust bearing was overloaded if the two different sections settled out at too high of a differential pressure. No other process conditions would overload the bearing. The bearing OEM performed a detailed analysis of the existing bearing which confirmed the physical results in the field. This allowed the creation of a unique thrust bearing design that increased the thrust capacity by approximately 40% without increasing the overall size of the thrust bearing. Since installation of the modified thrust bearing over a year ago, thrust position and bearing temperature during transient events have been substantially reduced.

SUMMARY

Two large refrigeration compressors at liquified natural gas (LNG) facility experienced several damaged thrust bearings in the past eight years, one of which caused a significant Lost Profit Opportunity (LPO) in 2017. During normal operation the load on the bearing is quite low. However, when the compressor shuts down, it experiences a rapid increase in thrust load due to the settle-out conditions inside the compressor. Increases in the discharge pressure of the compressor do not substantially increase the thrust load while running, but it greatly increases the transient thrust load. During the design phase of the compression package a dynamic simulation was not performed which could have identified the transient thrust load. A complete solution would be to install a hot gas bypass valve that would have quickly equalized the pressures in the compressor casing during shutdown. However, to install a valve of this size and nature would very difficult to justify and possibly extend the duration of the turnaround (TAR).

To improve the reliability of the compressors the following changes were implemented:

- A modified active thrust bearing with higher load capacity was installed on both compressors during 2022. The new bearing was a direct replacement of the existing bearing that required no housing modifications.
- The performance controller high discharge pressure limit control setpoints were lowered slightly. This change reduces the transient load on the bearing during shutdown, although calculations have shown that the pressure can still be high enough to fail the original bearing.

With these two changes, the compressors have operated since 2022 with less high temperature transients and no thrust bearing failures.

BACKGROUND

An LNG facility contained two identical compression trains each driven by a gas turbine and a helper motor. As is common with LNG facilities the compressor was rather large with a power requirement of approximately 45 MW. Because of space and arrangement limitations the decision was made during the design phase to combine the compressor into a two-section, back-to-back configuration (see Figure 1).

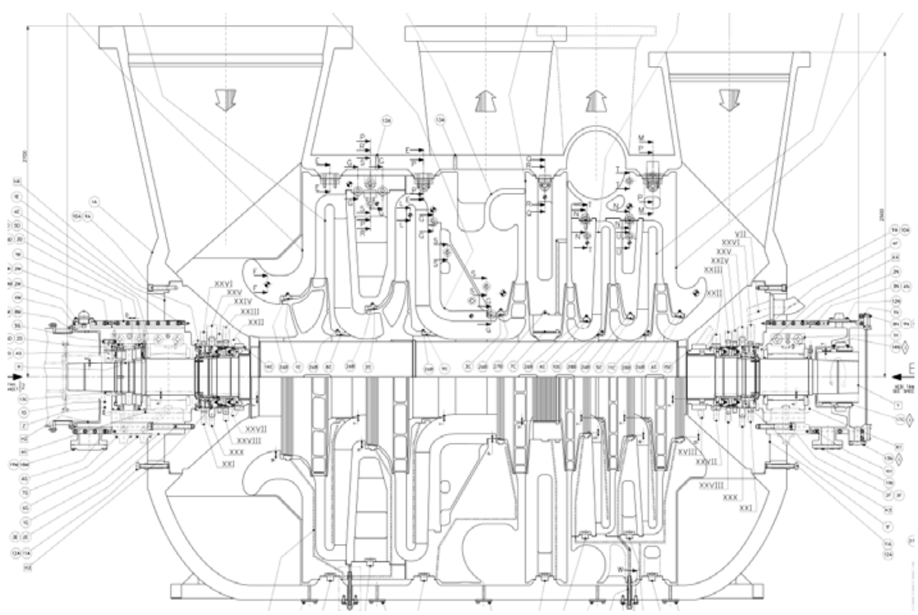

FIGURE 1. Cross-section of two section refrigeration compressor

In second quarter of 2015, a dry gas seal failure occurred on one of the refrigeration compressors requiring it to be shut down for repair. In the process of removing the dry gas seal it was discovered that the active thrust bearing had been damaged. The bearing had not failed, though the babbitt had started to wipe showing evidence of excessive load (Figure 2). This was a surprise, because there had not been any evidence of pending thrust bearing issues (i.e. temperature and axial position were both below alarm levels). The active side of the thrust bearing was replaced, and the compressor was re-started without incident.

FIGURE 2. Thrust bearing damage discovered during DGS replacement in July 2015

In April 2017, a process upset occurred which caused one of the Fr 7 refrigeration trains to trip. The remaining compression train went on total recycle, which caused all the suction and discharge pressure to increase. Eventually, this led to an active thrust bearing failure as is evident from the thrust position and temperature trends in Figures 3 and 4. The axial position increased from 0.3 to 1.25 mm (0.012 to 0.049 inches) (the designed total mechanical float was 0.5 mm (0.02 inches) and the active thrust temperature increased from 70 to 340°C (158 to 640°F)). The beginnings of the trends show how lightly the thrust bearing was normally loaded (i.e. 50% of the mechanical float and approximately 20°C (36°F) temperature rise). The rotor moved so far that all the babbitt was wiped from the thrust pads and the steel shoe contacted the thrust collar, damaging it as well (Figures 5-6). A root cause analysis (RCA) was conducted to determine the cause of the thrust bearing failure. Several root causes were considered and eliminated. The final root cause was never determined. As part of this RCA, the controls and operations procedures were modified to not allow the compressor to pressure up so much during plant process upsets. Also, plant feed was reduced earlier when one of the compression trains tripped to reduce the possibility of overloading the remaining train.

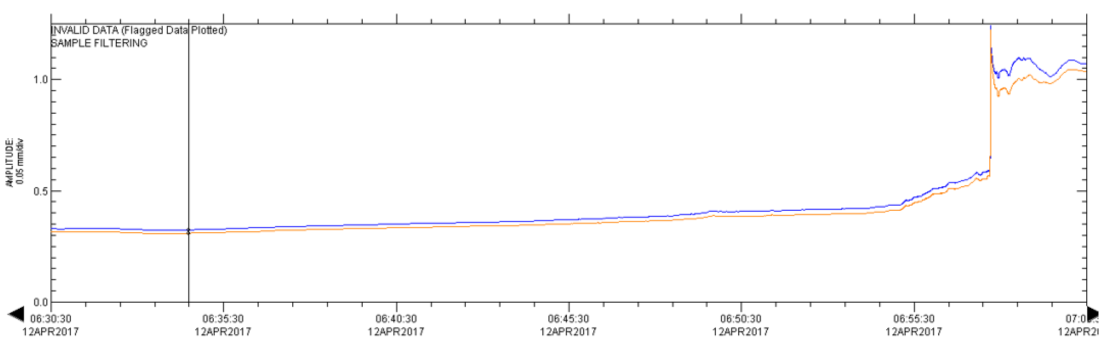

FIGURE 3. Trend of thrust position from 12 April 2017

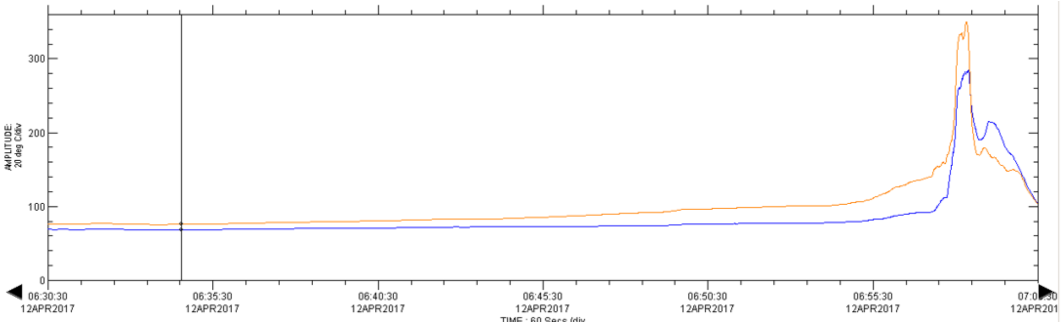

FIGURE 4. Trend of active thrust temperature from 12 April 2017

FIGURE 5. Failed active thrust bearing from April 2017 (close up on the right)

FIGURE 6. Damaged thrust collar from April 2017

In July of 2018, the LNG facility was brought down for a scheduled turnaround (TAR). Between the April 2017 failure and July 2018, the axial position and thrust temperature readings were normal, with the exception that both indications increased momentarily whenever the compressor shutdown. As part of the TAR, the thrust bearing was inspected to determine its condition. The mechanical float of the compressor was 0.05 mm (0.002 inches) above the maximum allowable and a visual inspection of the active pads showed that they had been heavily loaded and had started to wipe, see Figure 7. The active bearing pads were replaced, which returned the mechanical float within the allowable range. While the pads in these pictures are not close to failure, they do indicate that the bearing appears to be loaded much heavier than the axial position and thrust temperatures indicate. Additionally, they provide some additional clues to the possible cause of failure, which will be discussed in the next section.

FIGURE 7. Active thrust pads removed in July 2018 (close up on right)

THRUST BEARING FAILURE ANALYSIS

As mentioned earlier an RCA was completed in 2017 to help determine the cause of the thrust bearing failure. A full review of all the possible causes will not be listed; however, the three most likely causes of hydrodynamic bearing failures will be reviewed:

- Misalignment or installation error
- Insufficient lubrication
- Excessive load

The normal operating temperature of the bearing is approximately 70-75°C (158-167°F) with a 50°C (122°F) supply temperature, and the axial position ranges from 0.15-0.2 mm (0.006-0.008 inches). Since the mechanical float is approximately 0.5 mm (0.020 inches), this indicates that the thrust collar is only lightly loaded up against the active pad.

The original design consists of symmetrical equalizing thrust bearings prepared for direct lubrication. The design details are provided in Table 1.

Outer Diameter (OD)	419.1 mm (16.50 inches)
Inner Diameter (ID)	270.3 mm (10.64 inches)
Number of Pads	11
Pad Material	Steel
Bearing Type	Directed Lubrication, Leading Edge Groove (LEG) type
Surface Area	612.9 cm² (95 inch²)
Pivot Offset	60%
Pivot Diameter	28.4 mm (1.12 inches)
Pivot Height	12.7 mm (0.50 inches)
Oil Viscosity	ISO VG 32
Oil Supply Temperature	50°C (122°F)
Oil Flow (each)	100 Liters/min (26.4 GPM)

Table 1. Original Thrust Bearing Parameters

The active (counterclockwise (CCW) rotation) and inactive (clockwise (CW) rotation) subassemblies are equipped with three (3) platinum Resistance Temperature Detectors (RTDs) located at the 75/75 location (75% of the distance from leading to trailing edge, 75% of the distance from pad ID to OD).

MISALIGNMENT/INSTALLATION ERROR

The wear indications in all the inspections (Figures 2, 5, and 7) shows that all the pads appear to be carrying approximately the same load. Furthermore, there are no unusual bruises or asymmetric babbitt distress, and the wear patterns do not indicate an installation error. The low temperature rise and small axial position ranges at nominal operating conditions suggest that the bearing was installed correctly.

INSUFFICIENT LUBRICATION

Initial concern by the compressor OEM was that the bearing was somehow losing lube oil pressure on coast down (this theory also addressed why the temperature would spike on shutdown). Furthermore, it was determined that the size of the flow orifice on the thrust bearing supply had been changed since the original design from 32 to 25 mm (1.26 to 0.98 inches). However, flow calculations confirmed that the 25 mm (0.98 inch) orifice is large enough to supply the required flow rate, as determined by the bearing OEM. Additionally, a pressure transmitter was installed downstream of the orifice on the thrust bearing supply line which verified that the pressure does not drop during shutdown, see Figure 8. Further confirmation that adequate lubrication is present is the condition of the pads in Figure 7. Insufficient lubrication oil would result in burnt/varnished oil on the pads, however these pads only show evidence of higher load. Additionally, there are four other machinery casings in the train (one gas turbine, two other centrifugal compressors, and one helper motor) that all share the same lube oil system and none of them have had a bearing failure due to insufficient lubrication.

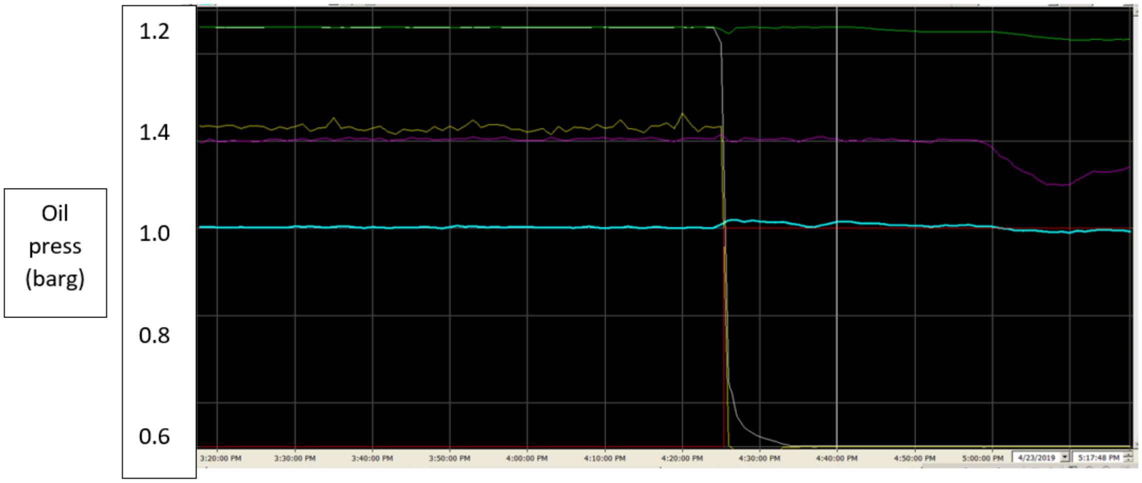

FIGURE 8. Lube oil pressure (light blue) when compression train shuts down, compressor speed (white)

EXCESSIVE LOAD

The original thrust bearing is rated for 249 kN (56,000 lbf), or 4.06 MPa (589 psi) loading. For this loading, at 3600 rpm, the predicted metal temperature is approximately 120°C (248°F). After the bearings were found to be damaged in July 2018, a revised investigation was started. The compressor OEM and operational engineers both calculated the gas load applied to the rotor which must be carried by the thrust bearing. These calculations were not just static pressures but included rotational pressure profile and change in momentum effects. None of the calculated thrust loads exceed the rated capacity of the bearing. Figures 5 and 7 are puzzling since the calculated thrust load (based on internal pressures and flows) during operation is very low.

The physical evidence from the thrust bearing damage as well as failures all point to excessive load [Blair and Pethybridge 2010]. One of the key pieces of evidence is the “crowning” effect that is evident in both Figures 5 and 7. Crowning is the deflection of the thrust pad around the pivot due to load. Figure 7 is especially noteworthy since it presents distress to high load prior to catastrophic failure. Figure 5 is the bearing appearance after a catastrophic failure, and clues are masked due to widespread damage and introduction of other distress modes. The bearing OEM did not have the opportunity to examine distressed bearing components, making Figure 7 especially valuable.

An example illustration of “crowning” is given in Figure 9. Nearly all hydrodynamic bearings experience crowning under load; it enables a center pivot bearing to develop a convergent oil film wedge [Raimondi and Boyd 1955, Greenwood and Wu 1995]. As can be seen in Figure 7, the outside peripheral of the bearing does not appear to be carrying any load. All the damage to the babbitt is localized to the area above and around the shoe support position. Note the 60% offset moves the pivot in the CCW direction. The babbitt temperature is always greatest at the trailing edge, and the hydrodynamic pressure greatest near the pad pivot [DeCamillo and Fabijonas 2012]. The fact that the calculated load before the April 2017 bearing failure is so low indicates that the bearing was probably already damaged prior to the rapid increase in thrust position and temperature.

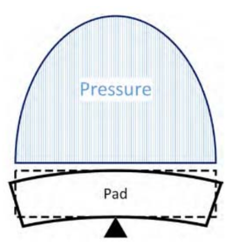

FIGURE 9. Crowning effect of thrust pads under load

As mentioned earlier, thrust temperatures always spiked when the compressor shutdown. High speed data acquisition was not available to record these spikes until the online vibration analyzer was repaired during the July 2018 TAR. Once the online analyzer was working, several transient events were recorded. Figure 10 shows a plot of axial position and active thrust temperature during a trip on 14 Jan 2020. At one point in the RCA, there was a large concern that higher thrust loads at very low speeds (< 500 rpm) might be causing the damage to the bearing. However, Figure 10 clearly shows that the thrust temperature drops off rapidly below 1000 rpm. The sharp speed and temperature decrease, combined with the smooth transition into a stabilized temperature, make additional bearing damage during this period unlikely.

	Ps(barg)/(psig)	Pd(barg)/(psig)	% Bearing rated capacity
Baseline	0.5/7.3	17.6/255.3	11
Max Flow	0.5/7.3	10.2/147.9	55
Before Apr 2017 failure	0.3/4.4	24.4/353.9	22

Table 2: Calculated thrust load for different design cases and April 2017 failure

Based upon the machine operating data and site test results, the bearing OEM used the assembled performance information to determine the approximate bearing load at the time of failure. A load value was required for continued evaluation, as well as ensuring a redesigned thrust bearing could accommodate the load without distress or failure. Confidence in a replacement bearing design could only be achieved with satisfactory performance predictions and an understanding of pad deflection during an upset event. The operating data provided presented in Figure 10 proved to be invaluable.

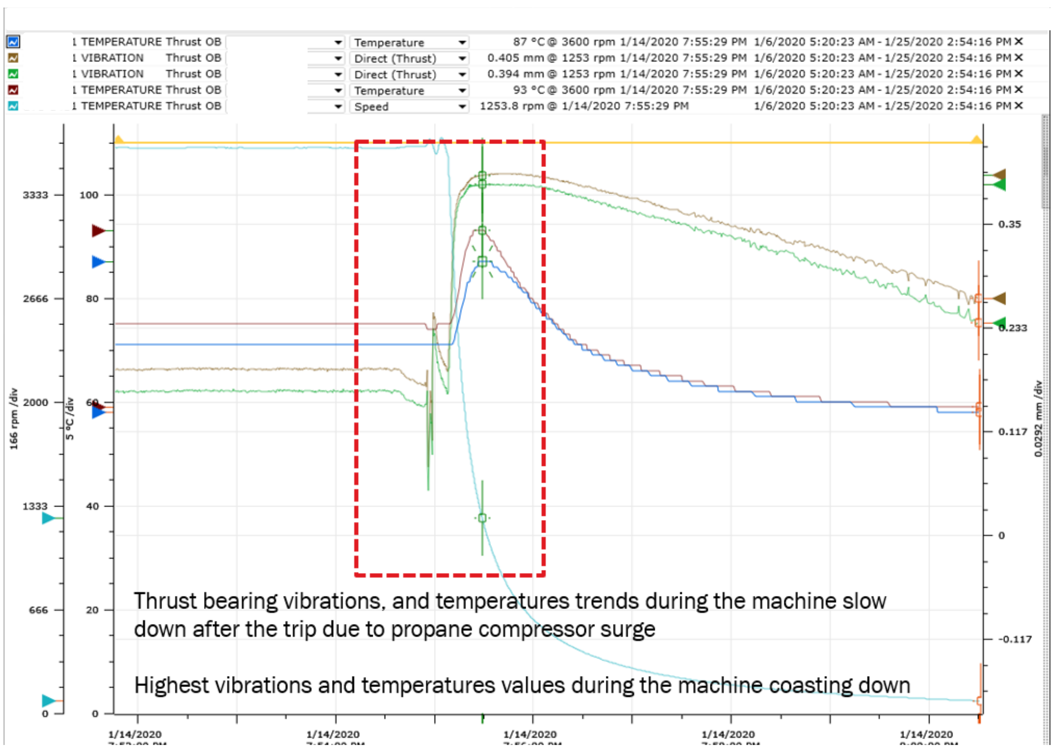

FIGURE 10. Compressor axial position and active thrust bearing temperature during trip on 14 Jan 2020

Referring to Figure 10, as the machine speed slowed to approximately 3000 rpm the thrust bearing temperatures sharply increased, indicating the onset of bearing distress. The bearing temperatures reached a maximum of approximately 93°C (200°F) as the rotor speed slows to 1250 rpm. This occurred approximately 21 seconds after the compressor trip. As stated above, the evidence at hand suggested bearing distress was created by high thrust load, but the source and magnitude were initially unknown. Information presented in Table 1 and Figure 10 was used to extract approximate load values at noteworthy transitions points. The bearing OEM relied on in-house code to identify the load required to generate temperatures measured during the upset event. The code is based on experimental results from extensive in-house high speed bearing testing. The analysis revealed a maximum load of approximately 320 kN (72000 lbf), or 5.2 MPa (758 psi) unit load (i.e. 128% of the rated load). Equipped with this information, a detailed evaluation of the load source and thrust pad design could begin.

SOURCE OF EXCESSIVE LOAD

This spike in axial position and thrust temperature is caused by a transient condition called settle-out that occurs on any compressor when it shuts down. When a compressor is running the gas pressure varies from suction to discharge inside the compressor and associated piping. However, when the compressor shuts down, the gas equalizes to one pressure that is based on the mass of gas inside the fixed volume of the compressor casing and piping. The compressor is a back-to-back compound configuration which is similar to having two compressors (Low Pressure (LP) and High Pressure (HP)) in one casing (Figure 11). During operation a small amount of gas leaks across the division wall seal between the two sections.

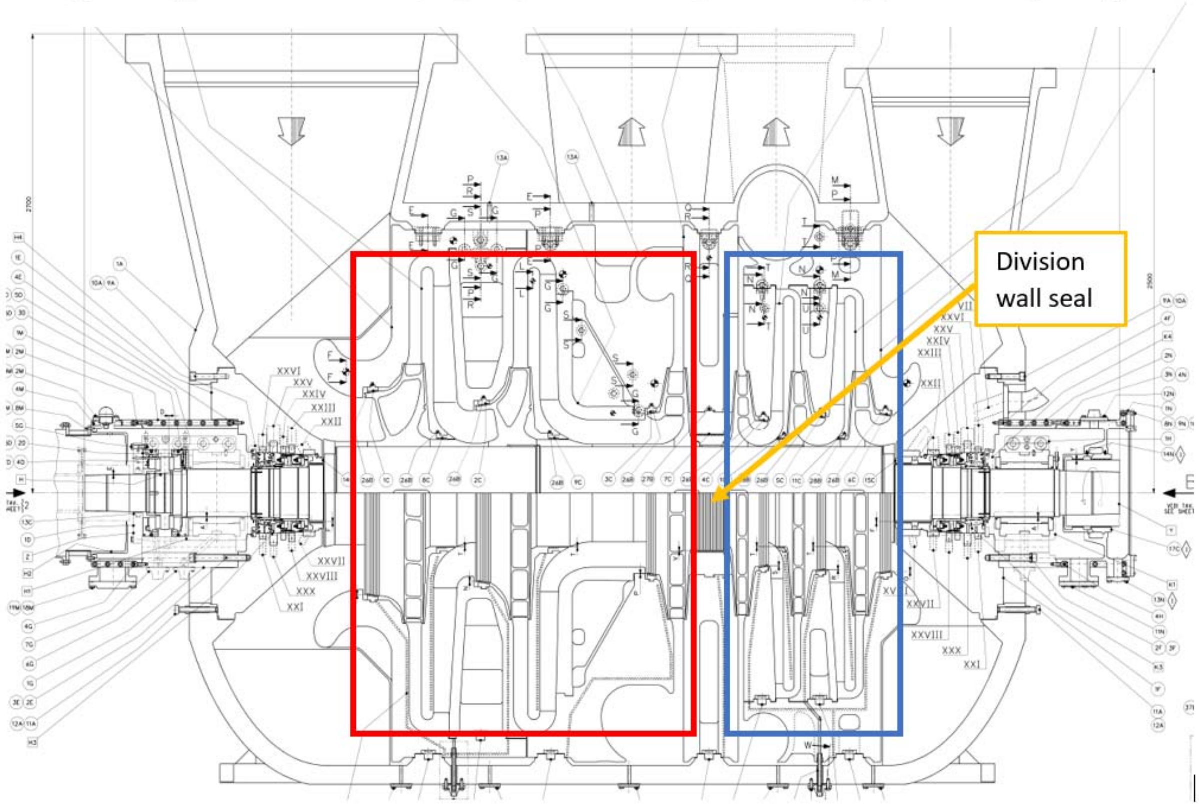

FIGURE 11. Cross-sectional drawing of compressor with LP (red) and HP (blue) outlined

When the compressor trips, all the gas in the LP section equalizes to one settle-out pressure, while the gas in the HP section equalizes to a higher settle-out pressure. At the same time, gas leaks across the division wall, and the two sections equalize to one common settle-out pressure. This transient event is graphically illustrated in Figure 12. The first settle-out to the two separate pressures occurs very rapidly, typically less than 10 secs. The subsequent combined settle-out can take much longer because it is controlled by the leakage rate across the division wall seal, not the thermodynamics of the gas.

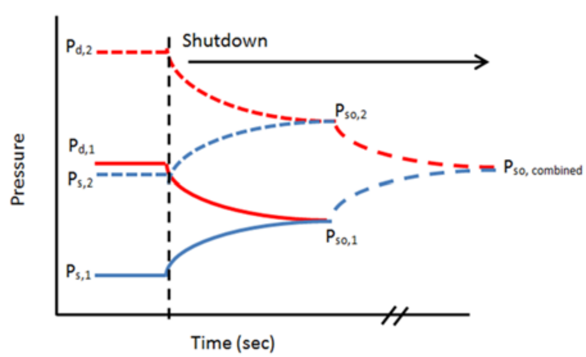

P_d	Discharge pressure
P_s	Suction pressure
P_{so}	Settle-out pressure

FIGURE 12. Typical settle out of compound compressor

The initial settle-out to two different pressures causes a high thrust load on the rotor pushing it in the active direction (right to left in Figure 11). High speed process data was obtained from the anti-surge controller for a trip of the compressor on 13 August 2017 (Figure 13). The gold line is the calculated thrust load and the green line is the speed. As described above, the peak thrust load occurs about 25 secs after the machine trips when the speed is approximately 1500 rpm. Notice the similarities between the thrust temperature in Figure 10 above and the calculated thrust load in Figure 13 below. The two trends are very representative of each other. A more severe trip occurred on the other compressor on 25 June 2017 when the HP discharge pressure was higher, see Figure 14. The large differential pressure between the LP and HP sections' settle-out pressures causes the peak thrust load to be much higher than that during normal operation.

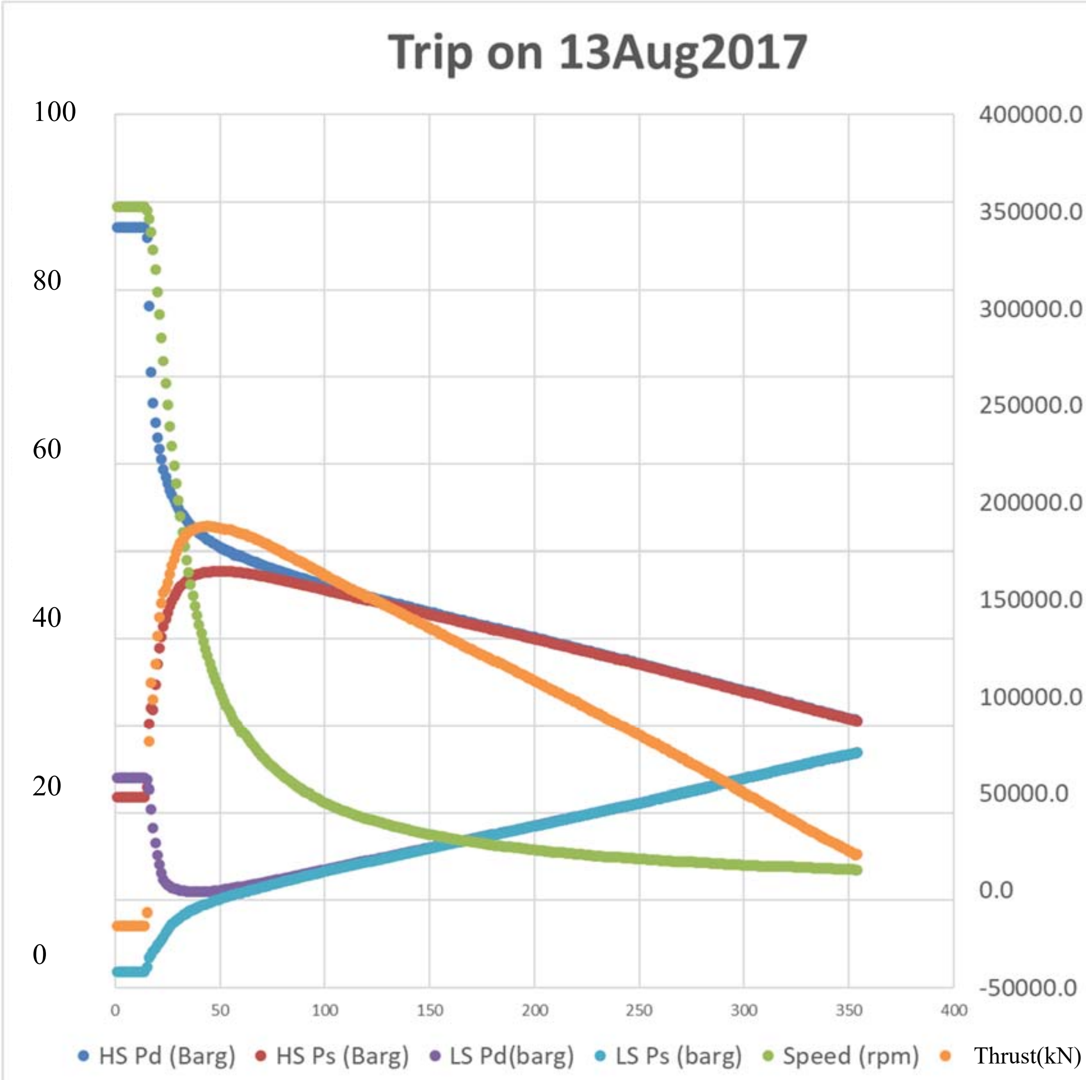

FIGURE 13. Compressor calculated thrust load (gold) and speed(green) based on 13Aug2017

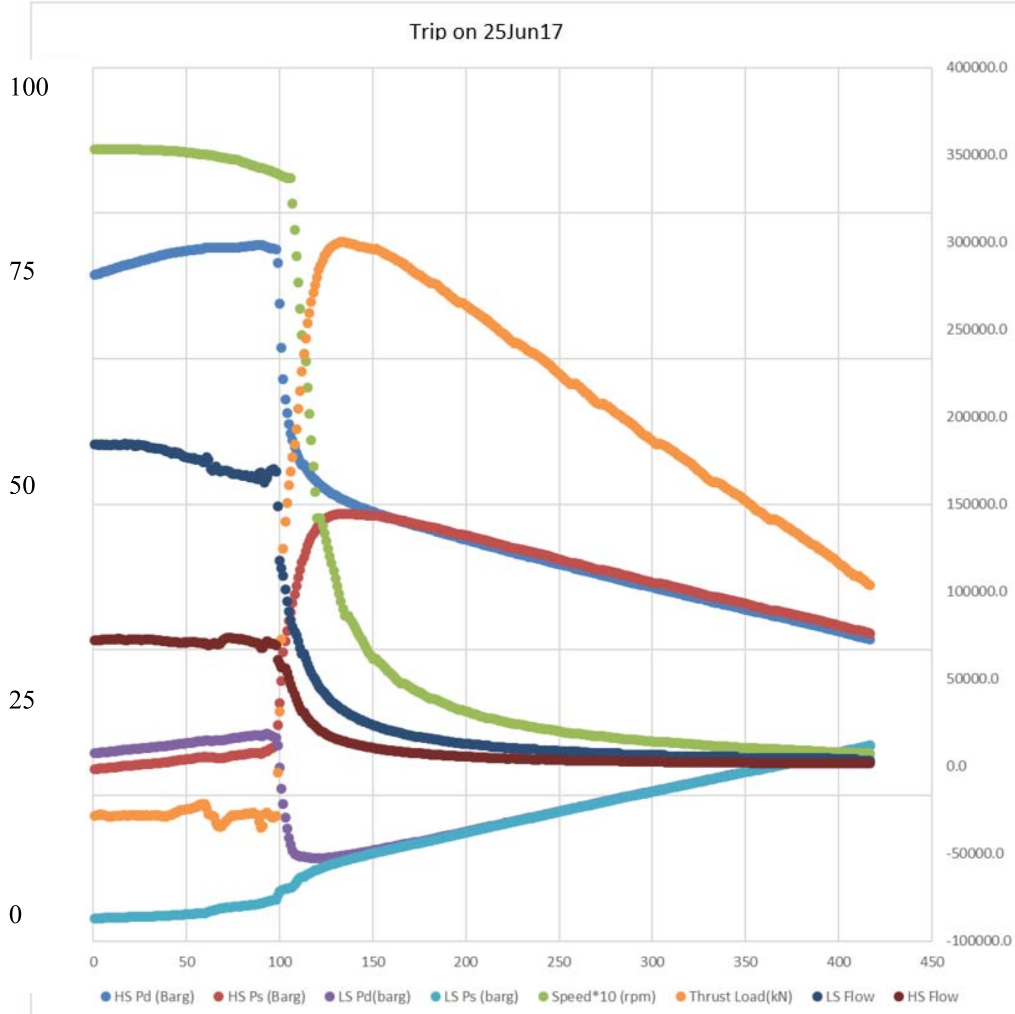

FIGURE 14. Compressor calculated thrust load (gold) and compressor speed (green) on 25Jun2017

The thrust load calculations for settle-out are much easier to calculate than when the compressor is running because the pressure is uniform in each section, which makes them more accurate as well. The thrust load is the difference in settle-out pressures multiplied by the area of the division wall seal. The calculation becomes so simple it can be represented by equation (1) which shows the approximate relation between the thrust loading expressed as percentage of the bearing capacity and the differential pressure (DP in barg) between the two sections at settle-out:

$$\% \, Thrust = 0.11 \times DP. \quad (1)$$

In summary, equation (1) shows that the thrust load exceeds the design capacity of the bearing whenever the differential settle-out pressure between the LP and HP sections exceeds 10 bar (145 psi). This equation was used with process data from several trips on both compressors in the past three years and showed that the thrust load had exceeded the bearing capacity on several occasions.

A further review of the thrust temperature shown in Figure 10 was made to compare the calculated thrust load from the pressure with the bearing OEM predictions of metal temperature for a given load. The process data from the Jan 14, 2020 trip was used to calculate the pressure load on the bearing and found to be 84% of the rated load or approximately 210 kN (47200 lbf). The bearing OEM was asked to predict the load required to produce a metal temperature of 93°C (200°F) at 1250 rpm. Their calculated value was 338 kN (76000 lbf) (135% of the thrust bearing capacity). This difference suggests that either the pressure load is greater than predicted or the bearing has already been damaged. An additional uncertainty exists in this comparison that would cause the difference between the two calculated loads to be even greater. The peak in thrust temperature in Figure 10 happens very quickly. If the load was held at this value for an extended period, the metal temperature would undoubtedly have gone up even more. Temperature measurements are normally only accurate during steady state events. This would result in an even higher calculated load.

Additionally, ever since the April 2017 bearing failure, operations personnel have reduced the load on the thrust bearing by making the following two changes:

- Process controls modifications – The pressure limit control setpoints have been lowered, which keeps the discharge pressure of both sections from rising too high. This was done to reduce the thrust load while the compressor is running but has the benefit of reducing the differential pressure between the two sections, which lowers the thrust load when the machine trips.
- Operational changes – Operational procedures are in place to pull feed from the plant when a refrigeration train starts to pressure up because it is overloaded. This keeps the discharge pressures lower as well, which limits the thrust load on shutdown.

These changes have certainly had a significant effect in reducing the damage to the thrust bearings in the years since the failure in 2017.

SOLUTIONS

INSTALLATION OF A HOT GAS BYPASS VALVE (HGBV)

The best solution to the high thrust load during the trip events is to reduce the load. This could be accomplished with the installation of a hot gas bypass valve (HGBV) illustrated in Figure 15. The HGBV rapidly equalizes the HP and LP section pressures when the compressor trips. This is very common on many offshore applications. However, it would be a very costly installation of a very large valve and piping. While a thrust bearing change would not be the total solution, if successful it would be much more cost effective than a HGBV. It is worth noting that the operator has another LNG facility with similar refrigeration compressors that do not have these issues because the two stages of compression are in *separate* casings which eliminates the high thrust load on shutdown.

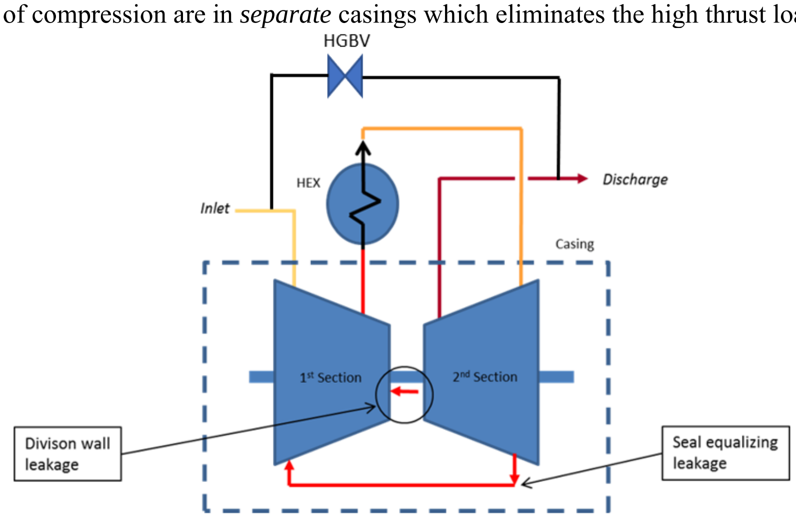

FIGURE 15. Compound compressor with Hot Gas Bypass Valve to reduce thrust load

NEW THRUST BEARING

The task that lay before the bearing OEM was to come up with a drop-in-place replacement that could handle the unexpected excessive load. As discussed above, the key issue was the pad crowning. Most tilt-pad fluid-film thrust bearing designs concentrate the load applied to the pad surface to a point or line contact at the pad-support-to-leveling-plate or pad-support-to-base-ring (in the case of non-equalizing designs) interface. The most notable exception is the design with spring-bed supports. The initial bearing had a catalog-sized pad-support diameter and depth within the pad. The excessive load forced the pad to crown around the support as well as crush the pad-support-to-leveling-plate contact. The bearing OEM's experience is that a larger, thinner pad-support can mitigate large deflections: by making the pad-support radius larger, the pad has less unsupported material to flex, especially when the pad-support is hardened; in making the pad-support thinner, the body of the pad becomes thicker and thus less prone to flex under load. There is, of course, a limit to these modifications: the pad must still be able to flex to some degree for normal operation, and enough material must remain for the pad-support to not lose integrity under load.

Although the maximum thrust load was estimated to be approximately 320 kN (72,000 lbf), the goal was to put in the largest and thinnest pad-support possible to better ensure a successful outcome. The solution is shown in Fig. 16. Details are presented in Table ~~2~~. 3

Outer Diameter (OD)	419.1 mm (16.50 inches)
Inner Diameter (ID)	270.3 mm (10.64 inches)
Number of Pads	11
Pad Material	Chrome Copper
Surface Area	612.9 cm² (95 inch²)
Pivot Offset	63%
Pivot Diameter	55.6 mm (2.19 inches)
Pivot Height	7.3 mm (0.29 inches)
Oil Viscosity	ISO VG 32
Oil Supply Temperature	50°C (122°F)
Oil Flow (each)	100 Liters/min (26.4 GPM)

Table 3. Redesigned Thrust Bearing Parameters

To study the effectiveness of this solution, the bearing OEM conducted a study of the shoe crown using a finite element thermo-elasto-hydrodynamic (TEHD) computer code which predicts bearing performance including temperature variation in the oil and pad as well as elastic and thermal deflection of the pad (Brockett, et al. 1996).

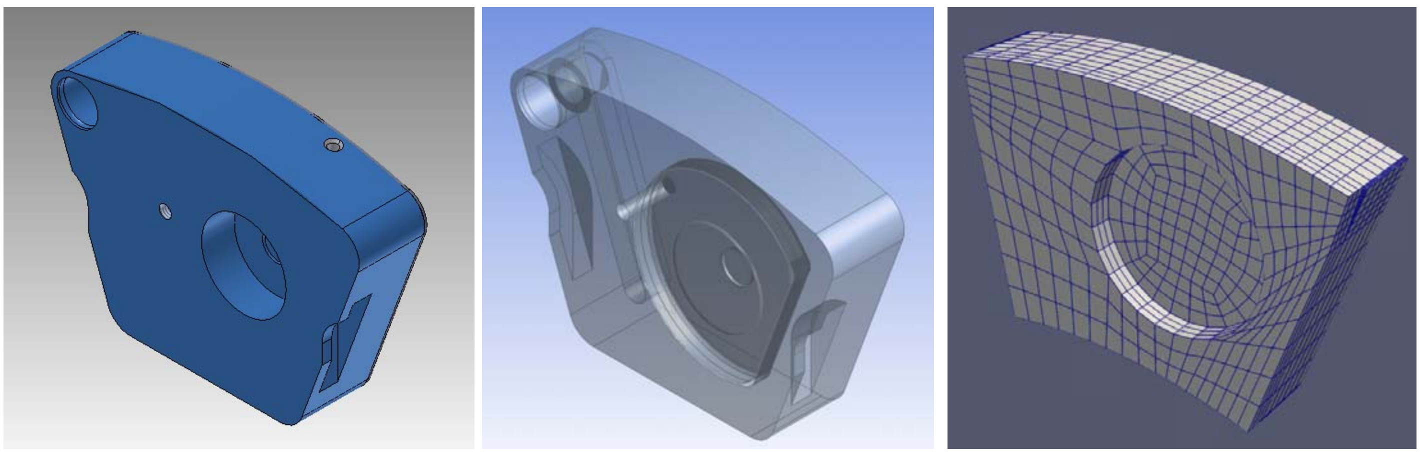

FIGURE 16: Sketch of the original shoe (left), the proposed solution (middle), and the computational model (right).

The TEHD code cannot directly simulate the suggested modification shown in the middle image of Fig. 16, particularly the truncated pad-support. What the program can model is shown in the right image of Fig. 16 without an LEG feed groove and with a full circular shoe support. We account for the lack of feed groove by choosing a moderate value (0.6) for the hot-oil-carryover factor. The allowable range of the pad-support radius in the TEHD code is 15%-35% of the pad radial width. The approach undertaken by the bearing OEM within the code's limitations was to simulate a sequence of pads with increasing shoe support diameter with the hopes of establishing a trend from which they could extrapolate the behavior of the real pad. The goal was to study how the pad crowned as described in Appendix A. Plotted in Figs. 17 and 18 are the ratios of pad crown to calculated minimum film thickness for a fixed load and speed and a sequence of shoe support radii from smallest (blue curve) to largest (purple curve). The curves are aligned to have zero pad crown at the center of the pad-support. The plots quantify the pad crown along the individual paths. The observed crown deviations over the pivot for large pad radii are artifacts of the model used in the TEHD code. These artifacts are small and have negligible effect on the solution. Finally, we caution the reader that the curves in Figs. 17-18 quantify the pad crowns and not actual deflection values.

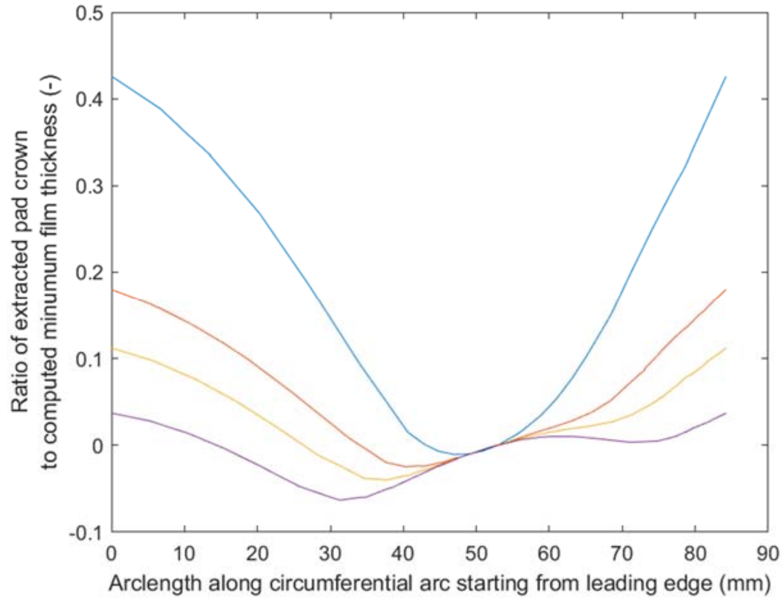

FIGURE 17: Ratios of pad crown to minimum film thickness along the circumferential path extracted from the TEHD code calculations for a sequence of increasing shoe support radii, where blue is the smallest and purple is the largest.

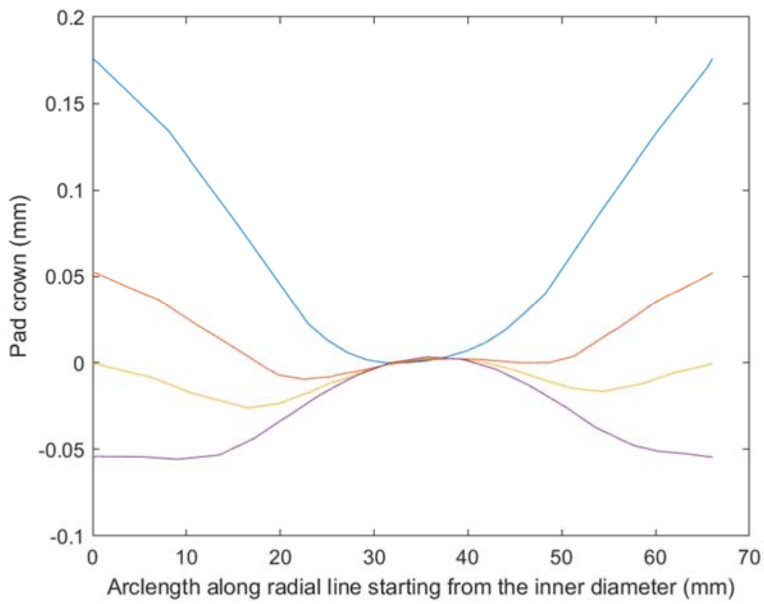

FIGURE 18: Ratios of pad crown to minimum film thickness along the radial path extracted from the TEHD code calculations for a sequence of increasing shoe support radii, where blue is the smallest and purple is the largest.

The trends in Figs 17-18 show that the pad crown reduces as the shoe support radius increases. Similar graphs for fixed pad-support radius and varying thicknesses also show that a similar trend—pad crown diminishes with the decrease in pad-support thickness. The bearing OEM extrapolated that that the design shown in Fig. 16 will have the smallest shoe crown.

After developing confidence in pad behavior under the high load condition, bearing operating performance was evaluated. As expected, predicted bearing operating temperatures dropped due largely to the material and pivot location changes. Additional benefits would have been achieved had the pad geometry allowed for a larger pivot offset. Referring to Fig. 16, the machined slots on the leading and trailing edges are used for pad retention in the bearing assembly. The existence of the slots and the need for large diameter supports prevented the offset from being greater. In order to achieve the 63% offset the trailing edge side of the support needed a straight edge. Regardless, there was no need to increase the offset. The primary purpose of the large diameter supports was to significantly reduce pad crowning during upset events.

RESULTS

The two modified active thrust bearings were installed during the TAR in July of 2022, see Figure 19 below. Since installation the thrust position and active thrust bearing temperatures have been significantly reduced. The compressors have operated through several process upsets without the bearing temperature or axial position entering the alarm level.

FIGURE 19. New thrust bearing (active side only) prior to installation in 2022

NOMENCLATURE

LNG = Liquid natural gas
RCA = Root cause analysis
TAR = Turnaround
LEG = Leading Edge Groove
LP = Low pressure
HP = High pressure
DP = Differential pressure
HGBV = Hot gas bypass valve
TEHD = Thermo-Elasto-Hydrodynamic

APPENDIX A

For the sake of simplicity, we examined the crown of the pad along two curves projected onto the surface of the pad as shown in Fig. A-1. The circumferential and radial paths pass through the center of the pad-support. Note that the peak pressure in Fig. A-1 is not located over the pad-support directly; rather, it is the center of pressure that is located over the pad-support. The pad deflection in the axial direction can be interpolated from the TEHD code's computation grid (Fig. A-2) onto these curves using common plotting software, e.g. ParaView (Ayachit 2015).

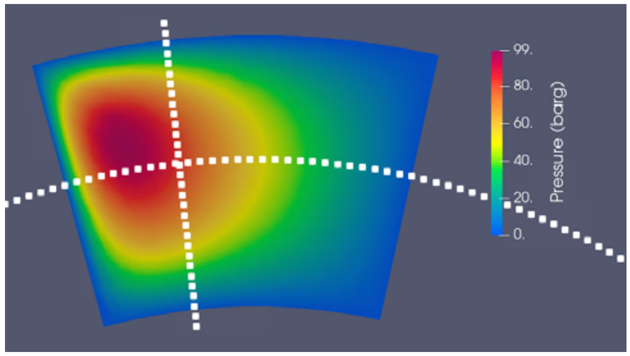

FIGURE A-1: Circumferential and radial paths along which the deflection field is extracted. The contours are those of the pressure field generated by the TEHD code for a 222kN load operating at 2200 rpm.

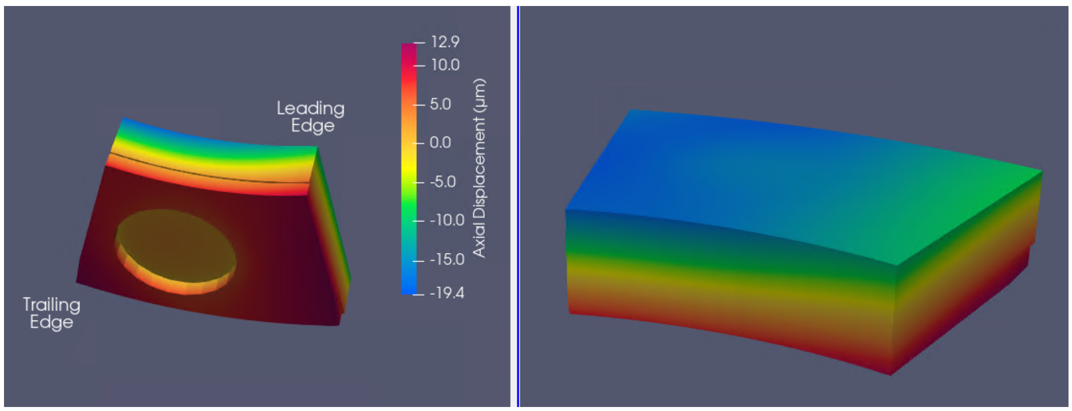

FIGURE A-2: Pad deflection data computed by THRUST corresponding to the operating conditions in Figure 17 as viewed from below (left) and above (right).

One now must extract the pad crown from the deflection data. Since we are looking at a converged solution in the code, the pad has undergone tilt and roll motions as well as thermal expansion and mechanical compression, all of which is reflected in the output data in Fig. A-2. The sign convention is defined by the code: positive values in Fig. A-2 correspond to deflections away from the pad surface toward the base ring, and negative ones correspond to deflections into the fluid domain. The top view in Fig. A-2 shows that most of the surface of the pad deflects into the fluid due to the zero-deflection boundary condition used by the TEHD code at the circumferential edge of the pad-support-to-pad-body interface. Consequently, the extracted raw data along the circumferential curve in Fig. A-1 is shown in the blue curve in Fig. A-3. The deviation of this data from a line connecting the two ends (orange line in Fig. A-3) is the pad crown (green arrows in Fig. A-3). Similarly for the radial curve. Note that the zero of the *x*-axis in Fig. A-3 starts at the leading edge of the pad; that is to say, the sense of rotation has been removed from the graph.

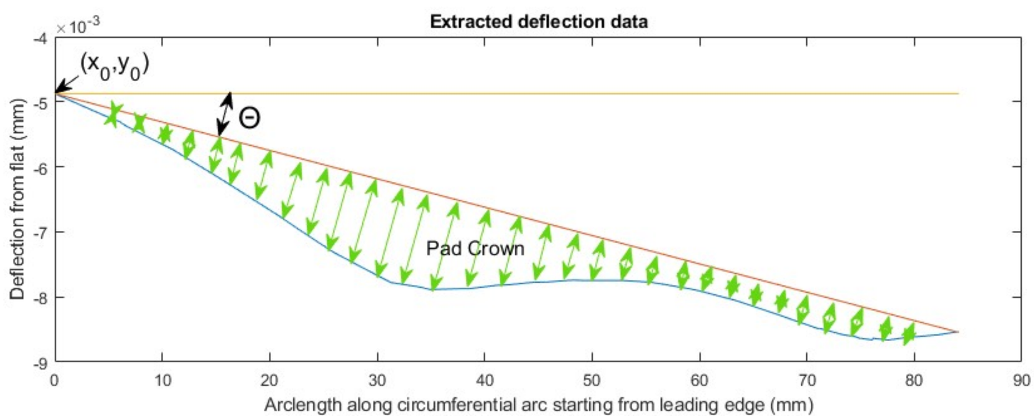

FIGURE A-3: Raw data of pad deflection extracted from the TEHD code as a function of arclength from the leading edge of the shoe.

Finally, it is beneficial to shift and rotate the data so that the orange line lies parallel with the *x*-axis:

$$\begin{pmatrix} x' \\ y' \end{pmatrix} = \begin{pmatrix} \cos\theta & \sin\theta \\ -\sin\theta & \cos\theta \end{pmatrix} \begin{pmatrix} x - x_0 \\ y - y_0 \end{pmatrix} - \begin{pmatrix} 0 \\ y_1 \end{pmatrix}.$$

Here, x_0, y_0, θ are depicted in Fig. A-3, and y_1 is a reference point on the pad to compare different crowns.

REFERENCES

Ayachit, Utkarsh, 2015, *The ParaView Guide: A Parallel Visualization Application*, Kitware, ISBN 9781630934306

Blair, B.J. and Pethybridge, G., 2010, "Hydrodynamic bearing damage and remediation of contributing factors in rotating machinery," *Proceedings of the of the 9th EDF/Pprime Poitiers Workshop*, Futuroscope, France, 14pp.

Brockett, T. S., Barrett, L. E., and Allaire, P. E., 1996, "Thermoelastohydrodynamic analysis of fixed geometry thrust bearings including runner deformation," Trib. Trans., 39, pp. 555–562.

DeCamillo, S.M. and Fabijonas, B.R., 2012, "Thrust Bearings", *Handbook of Lubrication and Tribology, Volume II: Theory and Design, Second Edition*, R.W. Bruce ed., CRC Press, Boca Raton, FL, 21pp.

Greenwood, J.A. and Wu, J.J., 1995, "Elasto-hydrodynamic lubrication of centrally pivoted thrust bearings," J. Phys. D: Appl. Phys., 28, pp. 2371-2377.

Raimondi, A.A. and Boyd, J., 1955, "The Influence of Surface Profile on the Load Capacity of Thrust Bearings With Centrally Pivoted Pads", Trans. ASME (J. Fluids Eng.), 77, pp. 321-328.

ACKNOWLEDGEMENTS

The authors thank their respective employers for permission to publish this work.